

# USING SURFACE EROSION OF AN ELECTRODE AS A METHOD TO MAP AND CHARACTERISE CAVITATION

CJB Vian      School of Chemistry, University of Southampton, Southampton, SO17 1BJ, UK  
PR Birkin     School of Chemistry, University of Southampton, Southampton, SO17 1BJ, UK  
TG Leighton   ISVR, University of Southampton, Southampton, SO17 1BJ  
B Zeqiri      Acoustics, Quality of Life Division, NPL, Hampton Road, Teddington, TW11 0LW  
M Hodnett     Acoustics, Quality of Life Division, NPL, Hampton Road, Teddington, TW11 0LW

## 1 INTRODUCTION

Cavitation is used in many industrial processes ranging from the processing of materials to surface cleaning. It is also used to destroy unwanted substances in large scale water treatment processes. While these useful effects have been harnessed, it is difficult to quantify cavitation within these processes<sup>1-3</sup>. Nevertheless it is possible to measure the effects of cavitation in many ways<sup>4</sup>; through methods utilising acoustic emission<sup>5,6</sup>, sonochemical change<sup>7,8</sup>, sonoluminescent light emission<sup>9,10</sup> and the destruction of materials. However, none of these methods are universally acceptable for a variety of reasons.

In 2000 the COMORAC (Characterisation Of Measures Of Reference Acoustic Cavitation) Experiment was devised and conducted by a team which included all but one of the current authors as key contributors<sup>11</sup>. In the COMORAC Experiment, researchers from 5 UK and one overseas centres were invited to a mostly unfamiliar laboratory (at the National Physical Laboratory) and given two days in which to use their favoured technique(s) for monitoring cavitation, to measure the amount of cavitation occurring in what was then the NPL's reference ultrasonic cleaning bath<sup>3</sup>. That test not only allowed cross-comparisons between techniques, but identified strengths and weaknesses in each. Subsequently, many of the techniques have been improved to ameliorate issues raised in the COMORAC Experiment. This paper represents one stage in this continuing process.

In the work presented here, the use of surface destruction recorded using a novel electrochemical technique is discussed. In particular a passive electrode surface is investigated and shown to be a useful technique for the mapping and characterisation of cavitation.

Cavitation bubbles are known to be either transient (termed inertial) or stable (termed non-inertial) depending on the physical conditions in their local environment<sup>4</sup>. At the low ultrasonic frequencies studies here, this dependency in practical terms depends primarily on the acoustic pressure, because it is not until higher frequencies that other factors achieve such importance (the sensitivity of the inertial cavitation threshold to the precise value of the frequency, and the initial bubble sizes present, become greater at, say, the MHz frequencies). Inertial cavitation events are described as having an isothermal expansion (to a value related to the initial bubble size,  $R_0$ , thought to be of the order of  $2-2.3 R_0$ )<sup>4,12</sup> followed by a rapid adiabatic collapse. This collapse is dominated by the inertial forces in the liquid and focuses the energy gained in the expansion phase into the collapsing gas bubble. As a result these events are known to produce high temperatures in the gas phase and the generation of shock waves<sup>4,13</sup>.

Consider individual cavitation events for the moment. It has been reported that if an individual inertial cavitation bubble of maximum radius,  $R_{max}$ , collapses close to a surface (distance between bubble and interface  $\leq R_{max}$ ), the implosion can damage the surface<sup>4,14</sup>. If however the cavitation occurs within a cloud of bubbles, the concerted collapse of that cloud can intensify the erosion generated at distance from the initial collapse<sup>4</sup>. In order to harness this cavitation erosion effect to form part of a sensing strategy, the material that the surface is made of can be selected so that it forms a passive protective film. Hence the subsequent erosion of this film is followed by the natural thermodynamically driven reformation. This reformation can be observed electrochemically

assuming that the electrode is maintained under electrochemical control<sup>10,15-17</sup>. Specifically, the reformation of this protective layer is observed as a rapid current spike (of the order of 100  $\mu$ s in duration although, as will be shown later, the exact timescale is dependant on the electrode material). This has already been observed and studied for several electrode systems (e.g. aluminium<sup>16,18</sup>, lead<sup>10,17</sup> and stainless steel<sup>18,19</sup>).

This work concentrates on the study of aluminium electrodes and the first use of titanium electrodes to observe surface cavitation events. It will be demonstrated that the choice of material has a significant effect on the events recorded and the lifetime of the sensor within an erosive environment. The inertial cavitation (or erosive) sensing electrodes are then employed to identify the standing wave effects (specifically the localisation of cavitation at acoustic pressure antinodes in standing wave fields which, for the vessel geometries studied here, produces concentric circles of luminescence or, if linear, produces 'banding'). This 'banding' of cavitation that can be seen within small cylindrical ultrasonic reactors<sup>9,20</sup>. Such localisation places requirements on the spatial resolution of the sensor. For example, a typical miniature hydrophone (Bruel and Kjaer 8103) has an active element measuring, hollow cylinder of diameter and height 6 mm, contained in a housing of 26 mm long and 9.5 mm in diameter. Such a sensor is therefore large and invasive with respect to the cavitation field (even if the hydrophone housing is made of rubber having the same acoustic impedance as pure water, it not only displaces regions of cavitation but also does not have the same acoustic impedance as bubbly water). In contrast the erosion electrode is physically smaller, displacing less of the cavitating field, and responds only over a small length scale (to be detected, the erosive cavitation event has to occur close to the electrode surface<sup>9</sup>). This length scale has been assessed for single cavitation events generated by a laser discharge into a liquid<sup>21</sup>. Philip and Lauterborn have suggested that the damage caused to the solid/liquid interface (note this damage is assessed through *ex situ* microscopy of the interface) has a complex relationship to the distance between the bubble centre and the solid/liquid interface<sup>21</sup>. This distance is assigned a dimensionless parameter,  $\gamma$ , which represents the ratio  $s / R_{max}$  where  $s$  is the distance between the bubble centre and the solid/liquid interface and  $R_{max}$  is the maximum bubble radius. In particular erosion as the result of primary bubble collapse occurs when  $\gamma < 1$  while erosion as the result of secondary collapse (after bubble rebound) occurs up to  $\gamma = 1.9$ <sup>21</sup>. However, it should be noted that these single bubble studies, although noteworthy, may not be totally relevant here. In acoustic multibubble environments, similar to those studied here, cavity cluster effects have been documented. These essentially increase the length scale over which erosion will be detected. Of course enhanced spatial resolution cannot be the sole goal of a cavitation detection system, since it does not cater to the requirement that a cavitation field be mapped out. Hence the electrode sensor system is deployed in conjunction with measurements of cavitation luminescence. The light detection system used in this paper has the advantage of real-time and simultaneous (i.e. without the need to scan) mapping of regions of activity in a cavitation field. However, luminescence imaging does have drawbacks. It is expensive, requires specialised black out conditions, and expertise in both deployment of the apparatus and in the interpretation of the results. For example scatter of cavitation luminescence from a non-cavitating surface should not be interpreted as a source of cavitation luminescence.

## 2 EXPERIMENTAL

Aluminium and titanium electrodes were fabricated by sealing wire (Advent Research materials 0.25 mm diameter purity: Al 99.98%, Ti 99.8%) inside a Pasteur pipette using slow set epoxy resin (Struers Epofix). Titanium electrodes were also made by thermally sealing the electrode material in soda glass (note this was not possible for aluminium because its melting point is below that of soda glass). Connections to all electrodes used shielded cable for the maximum possible length to reduce electrical noise from the ultrasonic equipment. Electrical connection between the electrode and the shielded cable was made using solder for aluminium and either silver paint or indium for titanium. The electrodes were polished to produce a smooth reproducible surface with successive grades of silicon carbide paper (400, 600 and 1200 Deer) and an alumina slurry (1  $\mu$ m and 0.3  $\mu$ m

Buehler) supported on Microcloth (Buehler). The electrodes were polished back to a smooth mirror like surface before each experiment.

In order to simplify the electrochemical apparatus employed, the electrodes were held at 0 V vs. a stainless steel or silver counter/reference electrode. A stainless steel needle was used as a counter/reference as this is a material commonly used for commercial baths. As a result, if the sensor is used in a bath it would be easy to set up the electrochemical circuit. The potential of the stainless steel bath *versus* a standard calomel electrode (SCE) in  $0.5 \text{ mol dm}^{-3} \text{ Na}_2\text{SO}_4$  was found to be -160 mV. A simple in-house current follower was used to amplify the signal. Current time transients were then recorded using either a Tektronix TDS 224 or a LeCroy 9310AM oscilloscope and the data transferred to a PC. To record and analyse data over a longer period of time, an Amptek Pocket MCA 8000A Multi Channel Analyser (MCA) was employed. This recorded the number and magnitude of peaks over a pre-determined period.

Microscopic images of the electrodes were taken using a Jai CV – A50 camera with 10 x microscope objective held 140 mm from the camera using lens stand off's. Low light images were taken using a Photek MCP325 intensifier with the intensified image recorded by a Jai CV-A50 CCD camera. All images were recorded using a Cyberoptics Imagenation PXC200A capture card in a PC. Averaging and stacking of multiple frames using Tambaware Software Image Stacker V 1.03 software were used to reduce noise in low light images.

Two different sources of cavitation were employed. In the first an Adaptive Biosystems ultrasonic horn operating at ~ 23 kHz was employed. This produced a localised and repeatable region containing inertial cavitation (in a region close to the face of the emitting surface). The electrode could then be positioned accurately (apparatus described elsewhere<sup>10,22</sup>) with respect to this sound source. The effects of cavitation and the subsequent erosion/corrosion processes could be studied<sup>19,22</sup>. In the second system, an in-house built ultrasonic cylindrical reactor was used. This reactor has a volume of 300 ml and is made of glass with a plastic base. The walls of the vessel are constructed using a water jacket to allow the temperature to be controlled. The reactor is driven by an MPIinterconsulting MPI-C-40 transducer with a resonant frequency of ~40 kHz. Both the ultrasonic horn and the reactor were driven by an electrical signal generated using a Thurlby Thandar TG1010 function generator and amplified by a Brüel & Kjear 2713 power amplifier.

All experiments were carried out in  $0.25 \text{ mol dm}^{-3} \text{ Na}_2\text{SO}_4$  (Fisher Scientific, Laboratory reagent grade), the water used was purified to  $>15 \text{ M}\Omega \text{ cm}^{-1}$  using an USF Elga Purelab Option E10 purification system. All chemicals were used as received. All experiments were performed at  $25^\circ\text{C}$  in aerobic solutions.

## 3 RESULTS

### 3.1 Horn experiments

The electrodes were positioned within a cavitation cloud produced by an ultrasonic horn using micropositioners (described elsewhere<sup>19,22</sup>). The inertial cavitation produced by this device has been shown to be within ~2 mm of the surface of the emitter<sup>15</sup>. Hence the electrode was generally positioned to within ~ 0.5 mm from the emitter surface. These conditions are thought to be suitable for the investigation of inertial cavitation events (generating both luminescence and surface events<sup>17,19</sup>). This allows the effects of inertial cavitation events above the surface of the electrodes to be easily studied. When an event occurs near to the electrode some of the passive layer of oxide is removed exposing the metal underneath to the solution and to the electrochemical environment. The oxide layer quickly reforms producing an anodic current spike. Such an erosion/corrosion event is shown in Figure 1. In this case a passivated aluminium electrode was employed. These transients, using aluminium, are considerably faster than those seen for similar systems such as lead which takes approximately  $60 \mu\text{s}$ <sup>17</sup> to return to 10 % of the maximum current in the transient compared to ~15  $\mu\text{s}$  seen here.

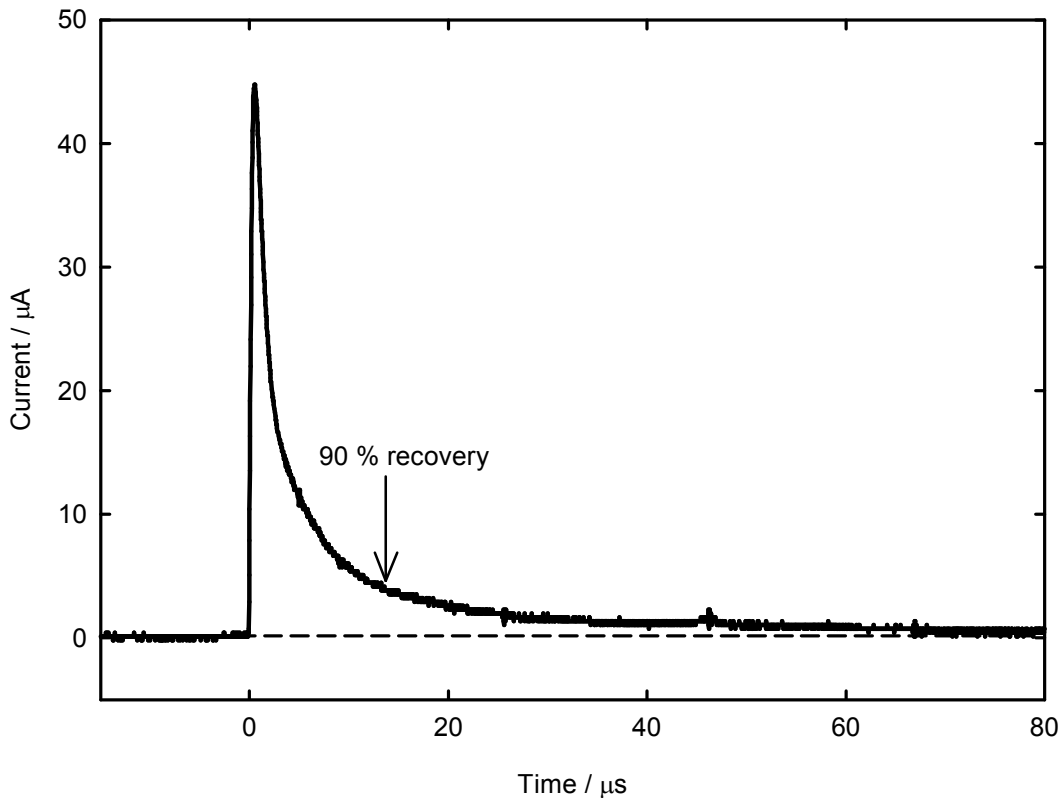


Figure 1: Plot showing a typical current time transient recorded for a surface event on an aluminium electrode (diameter 250  $\mu\text{m}$ ). The ultrasonic drive frequency was 23.17 kHz, voltage amplitude to the transducer was 100 V (zero to peak) corresponding to a power of  $56 \pm 5 \text{ W cm}^{-2}$  (calculated by Offin<sup>17</sup>). The electrode was positioned 0.5 mm from the tip of the ultrasonic horn.

After a period of prolonged exposure to these surface events caused by intense inertial cavitation ( $\sim 120 \text{ s}$ ), the surface of aluminium electrodes was found to become seriously deformed. The aging of the aluminium electrode is shown in Figure 2 as a function of exposure time. Figure 2 shows the damage to the surface of the electrode as easily visible pitting accompanied by the extrusion from the epoxy resin support of some of the aluminium. While this is not a direct problem for the sensor, it was noted that such an aged electrode starts to exhibit different characteristics to a polished electrode. This is manifested as the occurrence of numerous 'secondary events' being observed on the current time transients as well as the 'primary' events seen for a polished surface. Several such events are shown in Figure 3.

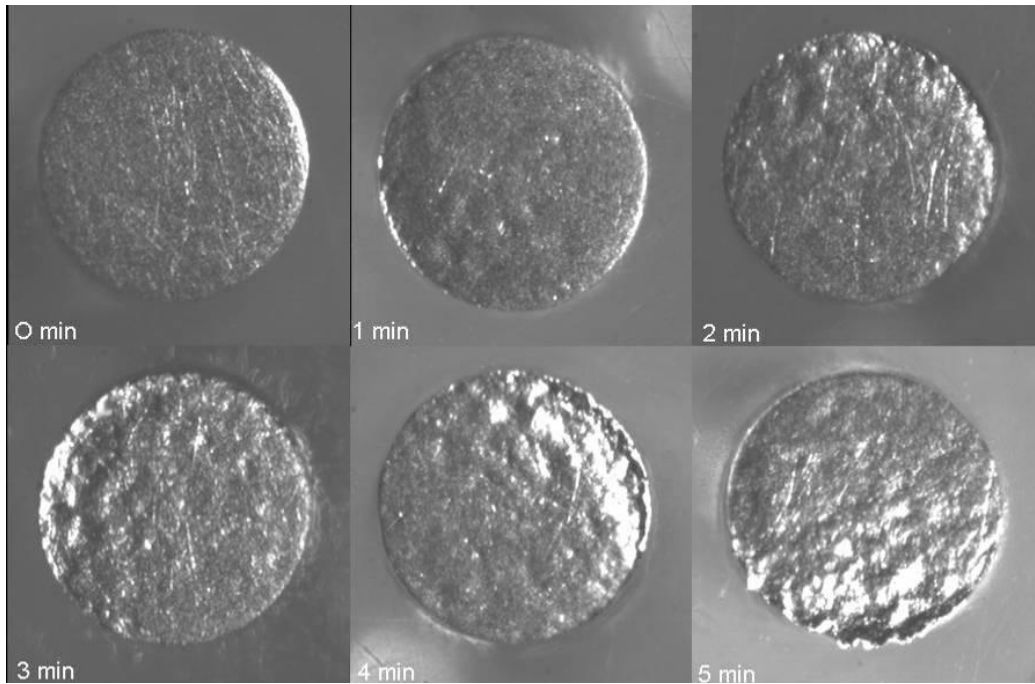


Figure 2: Showing the damage caused to the surface of the same aluminium electrode (diameter 250  $\mu\text{m}$ ) after 0, 1, 2, 3, 4 and 5 minutes held 0.5 mm from the tip of the ultrasonic horn. The ultrasonic drive frequency was 23.17 kHz, voltage amplitude to transducer was 100 V (zero to peak).

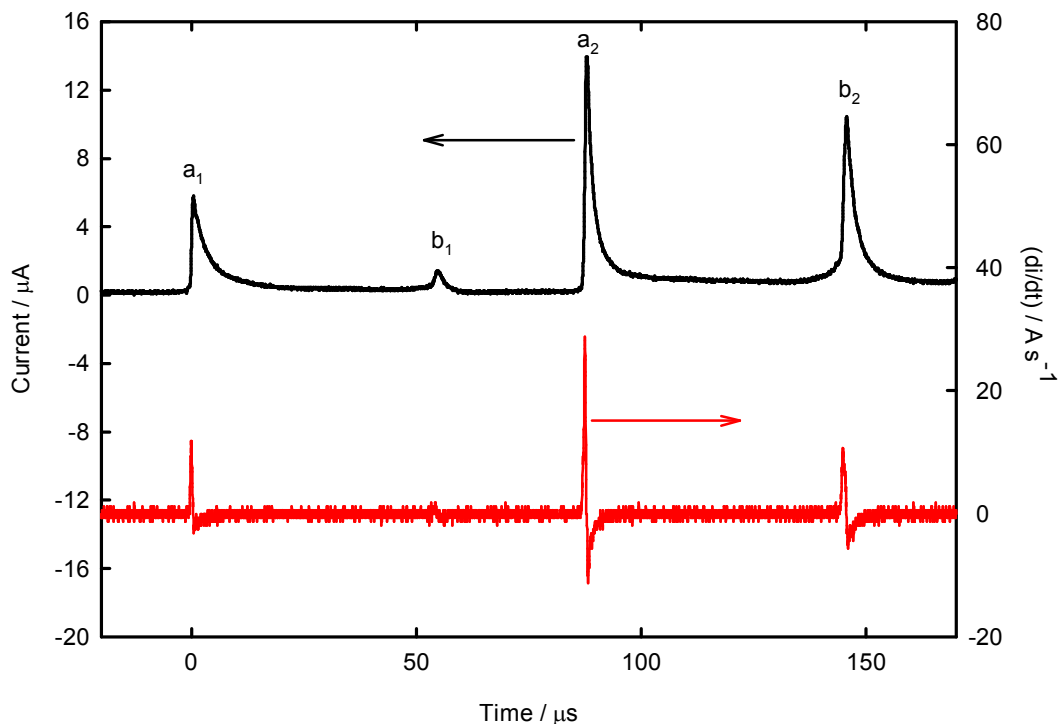


Figure 3: Current time plot (—) to show an example of the presence of slow rising 'secondary' transients ( $b_{1,2}$ ) as well as fast rising normal transients ( $a_{1,2}$ ) on an aluminium electrode (250  $\mu\text{m}$  diameter) after the surface has become damaged by the inertial cavitation events. The ultrasonic drive frequency was 23.16 kHz, voltage amplitude to the horn was 100 V (zero to peak). Included on the plot is the differential (—) with respect to time.

It should be noted that secondary events observed on these electrodes (labelled 'b<sub>1,2</sub>' in Figure 3) have a different shape to primary events (labelled 'a<sub>1,2</sub>' in Figure 3) which are observed for a pristine polished electrode. The origin of this change in behaviour is likely to be related to the aging of the surface. Such effects are currently under further investigation, but currently the hypothesis is that type 'a' events are the result of repassivation following rapid damage, such as fracture. Type 'b' events reflect the occurrence of slower processes which expose the substrate, such as plastic deformation: the exposure of fresh substrate is still occurring, ~10 microseconds after the repassivation begins, such that the rise time of the repassivation current is greater. This is emphasised in Figure 3 by the inclusion of the differential with respect to time. Here event 'a<sub>1</sub>' has a higher differential signal (11.875 A s<sup>-1</sup>) compared to 'b<sub>2</sub>' (10.625 A s<sup>-1</sup>) even though the current time trace for 'a<sub>1</sub>' has a smaller maximum when compared to 'b<sub>2</sub>'. Type 'b' events have not been observed when titanium electrodes are employed which is in accordance with this hypothesis. Clearly aluminium electrodes are able to record surface erosion events generated by acoustic cavitation. However, the extensive aging of this material which is manifested as additional events recorded on the surface (a process which could potentially lead to an over activity of the environment being detected) limits the use of aluminium as a sensing material. Hence further investigations concentrated on titanium which is considerably harder (titanium is 4.0 on the Mohs scale compared to 2.9 for aluminium<sup>23</sup>). Titanium, like aluminium, forms a passive oxide film when held at open circuit potential against either silver or stainless steel and consequently also produces anodic current spikes when subjected to inertial cavitation surface erosive events. These events, such as that seen in Figure 4, are generally smaller and longer in period than those recorded for aluminium (~200 μs to return to 10 % of the maximum current compared to ~ 60 μs for lead and 10-40 μs for aluminium electrodes). This makes them harder to detect (as higher gain equipment is required, typically 10<sup>5</sup> V A<sup>-1</sup> for Al compared to 10<sup>6</sup> V A<sup>-1</sup> for Ti) and record (as the electrode may not have fully recovered before the next event occurs over the surface). However, as can be seen from Figure 4A, the titanium electrodes are harder than the aluminium electrodes and therefore can withstand exposure to the inertial cavitation considerably better. This allows the titanium electrodes to be used for longer periods before becoming deformed and giving secondary current time events.

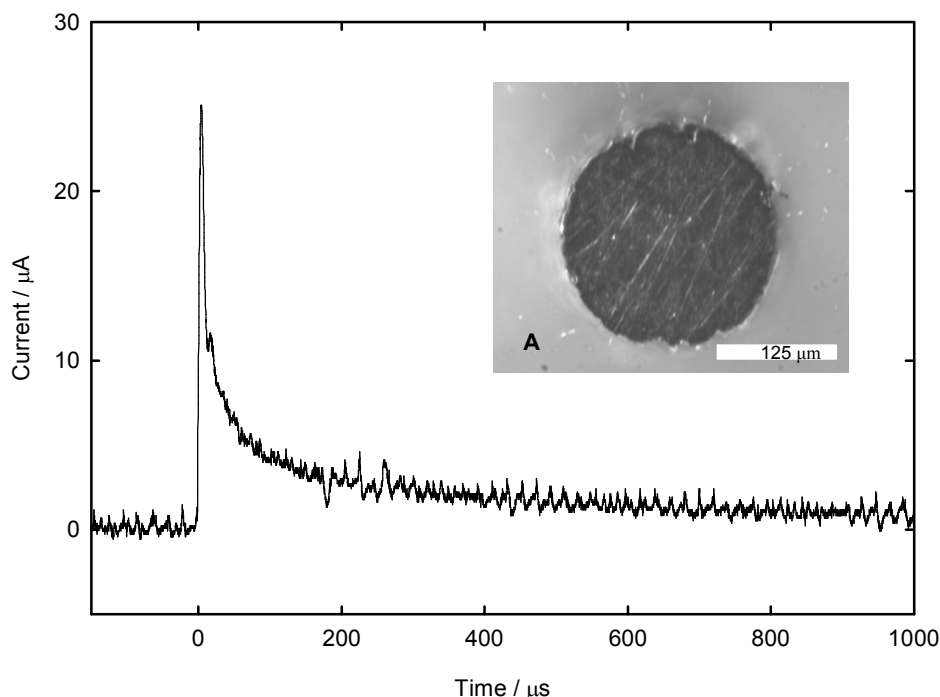


Figure 4: A typical transient from an inertial cavitation surface event on a titanium electrode (diameter 250 μm) positioned 0.5 mm from the tip of the ultrasonic horn. The ultrasonic drive frequency was 23.17 kHz, voltage amplitude to transducer was 100 V (zero to peak). Insert A shows the surface of the electrode after exposure to cavitation for 10 minutes.

The results presented thus far indicate that the measurement of inertial cavitation through erosion/corrosion of an electrode surface on both aluminium and titanium substrates have their uses. Aluminium electrodes are useful for systems where the production of inertial cavitation events is less frequent and so harder to detect. Under these conditions the surface will remain unperturbed for longer periods of time. However, titanium electrodes on the other hand are useful for higher intensity situations, where surface events are produced frequently within high intensity cavitation environments. In this situation the tougher material properties of Ti enable the electrode to behave as a sensor for longer periods of time, such that exposures of similar duration would cause the destruction and displacement of softer electrode materials (e.g. aluminium or lead).

It would be desirable to be able to compare the loss of material from electrodes with other detection techniques which rely on loss of material. This is currently not possible because of the small amounts of material involved. During a typical event, such as that in Figure 1, 257 pC of charge was passed. Using Faraday's law, the amount of oxide formed to replace that removed by the event is  $\sim 4.44 \times 10^{-16}$  moles. This corresponds to a mass of  $4.52 \times 10^{-14}$  g of  $\text{Al}_2\text{O}_3$ . It is interesting to compare this mass with the erosion of materials in mass loss experiments. In these cases a detection limit of the order of  $\sim 1$  mg can be found in the literature<sup>24</sup>. Comparing these numbers indicated that this electrochemical erosion/corrosion measurement is of the order of 11 orders of magnitude more sensitive. However, this is based on the comparison of a single cavitation event (the electrochemical measurement) with mass loss from many events<sup>24</sup>. For activity measurements it has previously been shown<sup>15,17</sup>, and will later be demonstrated in this manuscript, that between  $10$  and  $10^5$  electrochemical erosion/corrosion events can be used to monitor the spatial characteristics of inertial cavitation. Hence, it is likely that the erosion event can be used with a 6 orders of magnitude<sup>†</sup> increase in sensitivity compared to direct mass loss with a 1 mg resolution.

### 3.2 Surface events in an ultrasonic reactor

The previous discussion has shown that the detection of erosion/corrosion events can be useful in the characterisation of inertial cavitation. However, this detection/characterisation system must be capable of monitoring the spatial characteristics of inertial events within other environments. In order to demonstrate this, the detection system was deployed in an ultrasonic reactor. Whereas an ultrasonic horn produces a reproducible localised area of cavitation, an ultrasonic reactor has a cavitation field which is far more varied and frequency dependant. For example luminescent imaging of a cylindrical sonochemical reactor has shown that there are many regions of cavitation activity which are highly spatially dependant<sup>9,20,25</sup>. When such an environment is generated there are well defined areas of inertial cavitation activity. Using low light imaging techniques these areas can be observed from the multi bubble sonoluminescence (MBSL)<sup>1,4</sup> produced by inertial cavitation. These regions can be monitored using low light imaging techniques. In the cylindrical reactor employed here, the regions of the liquid where inertial cavitation exists can be defined. For example if the reactor is viewed from the side, a series of bands of light (see Figure 5a) can be recorded. However, if viewed from above concentric rings (see Figure 5b) will be observed. These perspectives are entirely expected and predictable given the three-dimensional structure of the mode<sup>25</sup>.

---

<sup>†</sup> The size and hence charge associated with the erosion/corrosion event will change this estimation. However, the calculation was based on a large anodic event (current maximum  $\sim 50$   $\mu\text{A}$ ) and can be considered as a worst case scenario. Hence this represents an underestimation of the sensitivity of the technique.

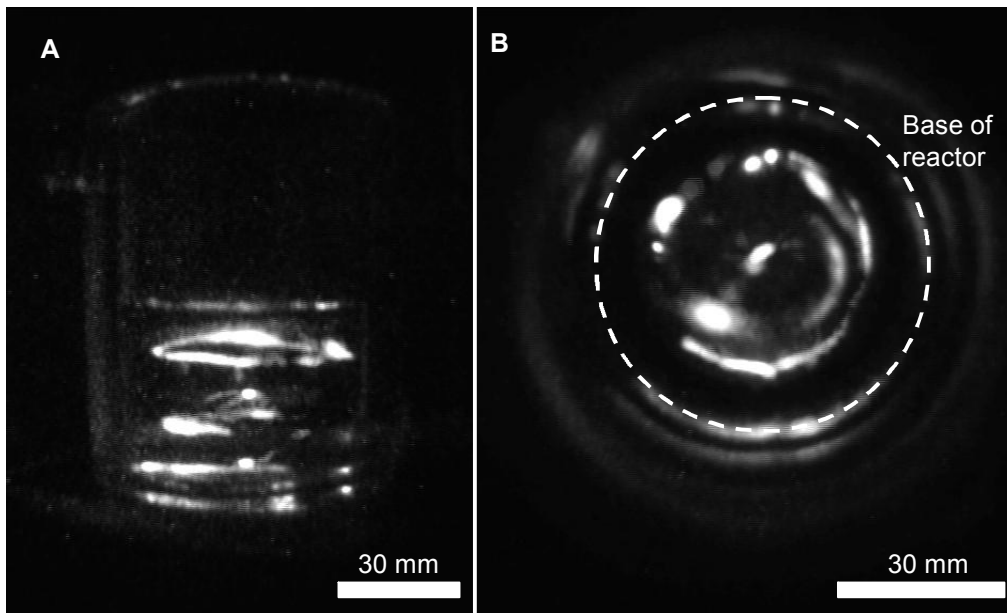


Figure 5: Low light images of ultrasonic reactor recorded from the side (A) and from above (B) showing banding (A) and concentric rings (B) formed from MBSL). Reactor contained 140 ml pure water and is driven at 40 kHz with a voltage of 100 V (zero to peak). Both images are averages of 100 individual images.

The high spatial resolution of the surface events technique presented here makes it suitable for investigation of this banding structure within a cylindrical reactor. It would be wrong to say that it represents the 'ideal' technique, because it cannot be used practically to map out the field as easily as can luminescence. To map the field, a single electrode would have to scan the 3D dimension of the cell, which is time-consuming (during which time the cavitation might change because of changes in the temperature, the gas content etc.). An array of electrodes capable of mapping to the degree allowed by the luminescence would be invasive. However the electrodes sensor represents a useful adjunct to the luminescence, capable of resolution within the bands.

In this initial feasibility study of the capability of the electrode sensor to undertake mapping of the band structure, the electrode can be positioned at different points within the reactor. For example if the electrode is positioned at different points in the vertical plane, the band structure should be evident as regions of zero activity (where the acoustic pressure is below the critical threshold for inertial cavitation<sup>25</sup>). In contrast regions of the liquid where the pressure exceeds the critical threshold pressure (e.g. at the pressure antinodes) will be detected by recording the number of erosion/corrosion events that take place at each point. In addition, further information may be acquired by monitoring the frequency and size of the erosion/corrosion events recorded. Hence the relative level of inertial cavitation activity can be found, even within a band which has a pressure amplitude above the inertial threshold. In order to demonstrate this, a mode was generated within a cylindrical reactor and an electrode placed in the centre of the cell and scanned vertically with a resolution of 2.5 mm. From the number of surface events recorded, using a multi-channel analyser, the presence of bands of inertial cavitation activity as can clearly be seen (see Figure 6).



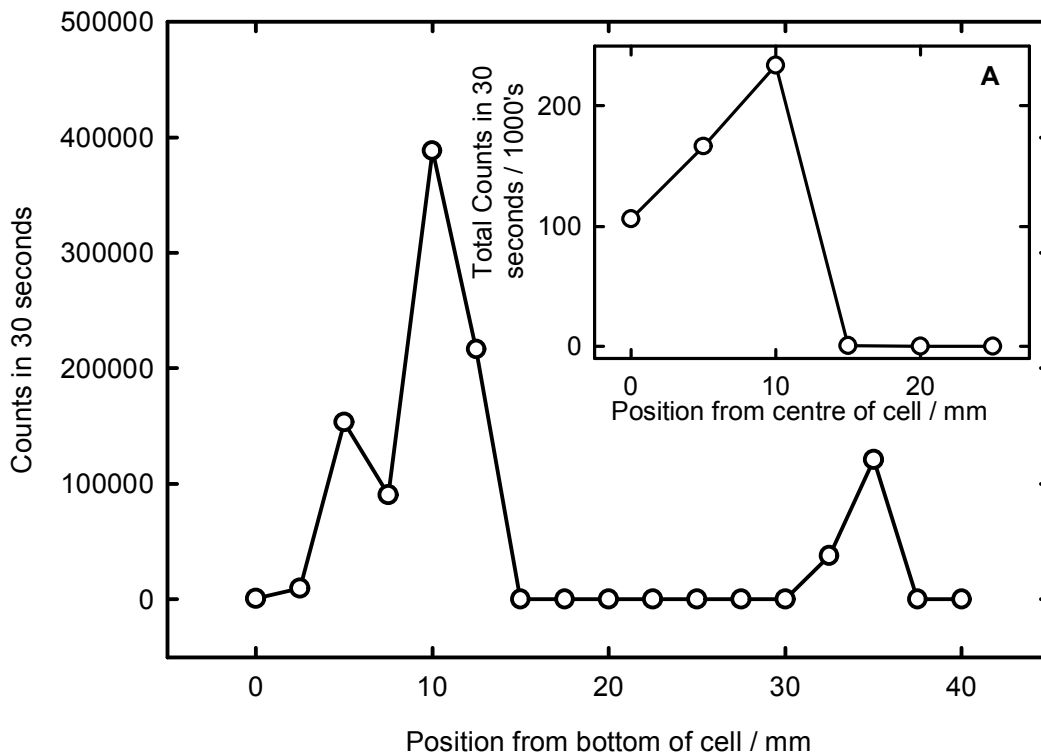


Figure 6: Variation in number of surface events recorded in 30 seconds as a function of vertical position within the reactor of a centrally placed electrode. Insert A shows the variation in the number of events as a function of horizontal position 7.5 mm above the base of the scan. MCA trigger set to channel 246 (0.3 V). 250  $\mu\text{m}$  aluminium electrode held at 0 V vs. silver wire and current follower set to  $10^5 \text{ V A}^{-1}$  gain. Reactor containing  $\sim 140$  ml solution driven at 40 kHz and 100 V (zero to peak amplitude).

Figure 6 shows that the bands of inertial cavitation activity are separated by  $15 \pm 2$  mm in the vertical direction. This compares to a spacing of  $13 \pm 2$  mm measured from the luminescent image (see Figure 5A). Similarly when an electrode was placed 7.5 mm from the bottom of a vertical scan (in a region where inertial events were detected in the centre of the cell) and then scanned horizontally across the reactor at 5 mm resolution, the horizontal activity was observed (see Figure 6 insert). This shows a ring like structure to the mode excited in the vessel. Figure 6 insert suggests that the inertial activity not apparent at the edge of the cell (close to the liquid/solid interface at the water jacket). It should be noted that the mode generated within the cylindrical vessel will have an influence on the interpretation of these scans. For example an asymmetrical mode will have pressure nodes on the axis of the cylinder while a symmetrical mode would have pressure antinodes on the axis. Hence care should be taken in comparing the activities measured using single line scans within the cell. Further characterisation using a 3D scanning technique would be required to fully characterise the shape of the erosive regions within the cell. These are currently under investigation.

#### 4 CONCLUSIONS

It has been shown that by using an electrochemical approach based on surface erosion/corrosion with either Al or Ti electrodes it is possible to map the relative level of inertial cavitation taking place within a system. The high level of spatial resolution that this technique affords allows for smaller reactors to be probed and for larger reactors to be investigated in greater detail. The use of two alternative electrode materials allows systems of differing cavitation activity to be investigated. Though not presented here, the results gained from surface event measurement can be correlated

with other techniques such as chemical dosimetry, photon counting and broadband noise emission towards generating a standard method for measuring cavitation. Finally a sensitivity gain of up to 6 orders of magnitude can be obtained using this technique in comparison with conventional weight loss measurements.

## 5 ACKNOWLEDGEMENTS

The authors acknowledge partial support of the work by the National Measurement System Directorate of the Department of Trade and Industry, under Project 3.4.1 of the 2004 - 2007 Acoustical Metrology programme.

## 6 REFERENCES

- 1 E. Neppiras, 'Measurement of Acoustic Cavitation'. IEEE Trans, Sonics Ultrason., SU-15(2): 81-88. (1968).
- 2 T.G. Leighton, A strategy for the development and standardisation of measurement methods for high power/cavitating ultrasonic fields: Review of Cavitation Monitoring Techniques. 263, ISVR, University of Southampton. (1997).
- 3 T.G. Leighton, P.R. Birkin, M. Hodnett, B. Zeqiri, J.F. Power, G.J. Price, T. Mason, M. Plattes, N. Dezhkunov and A.J. Coleman. 'Characterisation Of Measures Of Reference Acoustic Cavitation (COMORAC): An experimental feasibility trial'. In: A.A. Doinikov (Editor), Bubble and Particle Dynamics in Acoustic Fields: Modern Trends and Applications. Research Signpost, Kerala, India, 37-94.(2005)
- 4 T.G. Leighton, 'The Acoustic Bubble', 1st ed. Academic Press Inc, San Diego, 613 pp. (1994).
- 5 B. Zeqiri, P.N. Gelat, M. Hodnett and N.D. Lee, 'A novel sensor for monitoring acoustic cavitation. Part I: Concept, theory, and prototype development'. IEEE Trans. Ultrason. Ferroelectr. Freq. Control, 50(10): 1342. (2003).
- 6 B. Zeqiri, N.D. Lee, M. Hodnett and P.N. Gelat, 'A novel sensor for monitoring acoustic cavitation. Part II: Prototype performance evaluation'. IEEE Trans. Ultrason. Ferroelectr. Freq. Control, 50(10): 1351. (2003).
- 7 P.R. Birkin, J.F. Power, T.G. Leighton and A.M.L. Vincotte, 'Cathodic electrochemical detection of sonochemical radical products'. Anal. Chem., 74(11): 2584. (2002).
- 8 G.J. Price, F.A. Duck, M. Digby, W. Holland and T. Berryman, 'Measurement of radical production as a result of cavitation in medical ultrasound fields'. Ultrason. Sonochem., 4(2): 165. (1997).
- 9 J. Power, Electrochemical, Photographic, Luminescent and Acoustic Characterisation of Cavitation. PhD Thesis, University of Southampton, (2003).
- 10 P.R. Birkin, D.G. Offen and T.G. Leighton, 'Electrochemical measurements of the effects of inertial acoustic cavitation by means of a novel dual microelectrode'. Electrochem. Commun., 6(11): 1174. (2004).
- 11 T.G. Leighton, 'Characterization of measures of reference acoustic cavitation (COMORAC)'. J. Acoust. Soc. Am., 108(5): 2516. (2000).
- 12 R.E. Apfel, 'Possibility of Microcavitation from Diagnostic Ultrasound'. IEEE Trans. Ultrason. Ferroelectr. Freq. Control, 33(2): 139. (1986).
- 13 C.K. Holland and R.E. Apfel, 'An Improved Theory for the Prediction of Microcavitation Thresholds'. IEEE Trans. Ultrason. Ferroelectr. Freq. Control, 36(2): 204. (1989).
- 14 B. Vyas and C.M. Preece, 'Stress produced in a solid by cavitation'. J. App. Phys., 47(12): 5133-5138. (1976).
- 15 P.R. Birkin, D.G. Offen and T.G. Leighton, 'Experimental and theoretical characterisation of sonochemical cells. Part 2: cell disruptors (Ultrasonic horns) and cavity cluster collapse'. Phys. Chem. Chem. Phys., 7(3): 530-537. (2005).
- 16 P.R. Birkin, R. O'Connor, C. Rapple and S. Silva-Martinez, 'Electrochemical measurement of erosion from individual cavitation events generated from continuous ultrasound'. J. Chem. Soc.-Faraday Trans., 94(22): 3365. (1998).

- 17 D.G. Offin, Acoustoelectrochemical characterisation of cavitation and its use in the study of surface processes. PhD Thesis, University of Southampton, Southampton, (2006).
- 18 S. Silva-Martinez, Applications of Ultrasound in Electrochemistry. PhD Thesis, University of Southampton, Southampton, (1997).
- 19 P.R. Birkin, T.G. Leighton and D.G. Offin, 'The study of surface processes under electrochemical control in the presence of inertial cavitation'. *Wear*, 258: 623-628. (2005).
- 20 P.R. Birkin, J.F. Power, M.E. Abdelsalam and T.G. Leighton, 'Electrochemical, luminescent and photographic characterisation of cavitation'. *Ultrason. Sonochem.*, 10(4-5): 203. (2003).
- 21 A. Philipp and W. Lauterborn, 'Cavitation erosion by single laser-produced bubbles'. *J. Fluid Mech*, 361: 75-116. (1998).
- 22 P.R. Birkin and S. Silva-Martinez, 'A study of the effect of ultrasound on mass transport to a microelectrode'. *J. Electroanal. Chem.*, 416(1-2): 127-138. (1996).
- 23 'Smithsonian Physical Tables', 9<sup>th</sup> Revised ed. Knovel, 837 pp. (2003).
- 24 A. Shima, T. Tsujino and H. Nanjo, 'Nonlinear Oscillations of Gas-Bubbles in Viscoelastic Fluids'. *Ultrasonics*, 24(3): 142-147. (1986).
- 25 P.R. Birkin, T.G. Leighton, J.F. Power, M.D. Simpson, A.M.L. Vincotte and P.F. Joseph, 'Experimental and theoretical characterization of sonochemical cells. Part 1. Cylindrical reactors and their use to calculate the speed of sound in aqueous solutions'. *J. Phys. Chem. A*, 107(2): 306. (2003).